Monitoring the Orbital Decay of the Chinese Space Station Tiangong-1 from the Loss of Control until the Re-Entry into the Earth's Atmosphere

Carmen Pardini[a1]*, Luciano Anselmo[a2]

[a] *Space Flight Dynamics Laboratory, Institute of Information Science and Technologies (ISTI), National Research Council (CNR), Via G. Moruzzi 1, 56124 Pisa, Italy*

[1] carmen.pardini@isti.cnr.it; [2] luciano.anselmo@isti.cnr.it

[*] *Corresponding Author*

Abstract

Launched in September 2011, the first Chinese space station Tiangong-1 was originally planned to be deorbited with a controlled re-entry at the end of its operational life. However, due to a fatal on-board failure that occurred in March 2016, it was irremediably doomed to an uncontrolled decay. The latter was regularly monitored at ISTI-CNR, which also joined an international re-entry campaign, starting a couple of months before the final decay, on 2 April 2018, apart from providing support to the Italian Space Agency for the National Department of Civil Protection.

In spite of numerous challenges encountered during the campaign, due to the complex dynamics of the re-entering object, due to the lack of information on its structure and fragmentation process, and due to the distinctive characteristics of the space environment, often not properly represented by the available semi-empirical thermosphere density models, reasonable and conservative solutions were devised and applied, providing a valuable support to plan, at national level, the appropriate measures to mitigate the potential risk to airspace and on the ground due to falling debris from this uncontrolled re-entry.

Keywords: Tiangong-1, Chinese space station, uncontrolled re-entry, re-entry campaign, re-entry predictions, re-entry risk.

1. Tiangong-1

Tiangong-1, whose name translates as "Heavenly Palace 1", was the first Chinese space station and blasted off on 29 September 2011 aboard a Long March 2F rocket, launched from the Jiuquan Satellite Launch Center, in the Gobi Desert. As a precursor to a full-scale modular station, which China is planning to complete by the early 2020s, Tiangong-1, placed in a nearly circular orbit with an altitude of about 350 km and inclination just less than 43°, was used to test docking and rendezvous techniques, and to host two crewed missions.

In November 2011, the unmanned spacecraft Shenzhou-8 reached the station, executing the China's first-ever orbital docking. Seven months later, in June 2012, the docking was repeated by three Chinese astronauts with their Shenzhou-9 spacecraft. The station was visited again, and for the last time, in June 2013, when the Shenzhou-10 spacecraft transported another trio of astronauts. Each of these crewed missions lasted about two weeks.

Tiangong-1was about 10.4 m long by 3.4 m wide, and it weighed about 8.5 metric tons at liftoff. The space laboratory consisted of two main parts: a 2.8 m diameter service module that accommodated the propulsion and electrical systems, and a 3.35 m orbital module that housed the visiting astronauts. With its two rectangular solar panels deployed, Tiangong-1 had a wingspan of 17 m (see Figure 1).

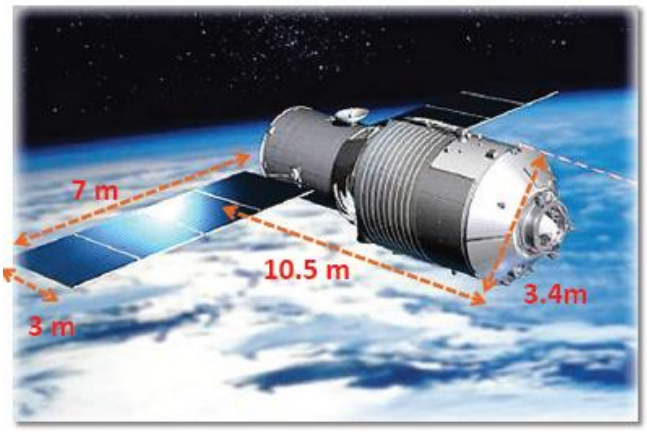

Fig. 1. The Chinese space station Tiangong-1 (courtesy of the China Manned Space Agency).

Tiangong-1 was originally planned to be deorbited in 2013, after two years of operations and the completion of a series of technological tests, being replaced by Tiangong-2, a similar but improved laboratory. The controlled re-entry was foreseen in the South Pacific Ocean Uninhabited Area (SPOUA). However, China repeatedly extended the length of the Tiangong-1 mission until 16 March 2016, when ground controllers lost the contact with the vehicle, likely due to an on-board fatal power failure. After a while, China reported that their space station had "ceased functioning" on 16 March 2016, without specifying the reason. Finally, in September 2016, Chinese officials confirmed that the space station was heading for an imminent re-entry after suffering an on-board failure in March, but they did not disclose whether the spacecraft descent was controlled or not. At that time, the first announcements made by the Manned Space Engineering Office of China (CMSEO) indicated that Tiangong-1 was descending for its fiery plunge into the Earth's atmosphere in late 2017. Such delay in the re-entry led some experts to suspect that the space laboratory was out of control, and that the latter could not be regained.

One year later, in May 2017, China informed the United Nations Office for Outer Space Affairs (UNOOSA) that the operational orbit of the vehicle was "under constant and close surveillance by China", that the average altitude of the space station was around 349 km, and that it was decaying at a rate of approximately 160 m/d. Under these conditions, the re-entry of Tiangong-1 was expected sometime between October 2017 and April 2018 [1]. This note also stated that the dynamical orbital status and other information related to Tiangong-1 would have been posted on the website of the China Manned Space Agency (www.cmse.gov.cn).

2. Risk of the uncontrolled re-entry

Tiangong-1 was one of the most massive objects to re-enter without control in the second half of the 2010s, but it was by no means the largest ever. In terms of mass it was in fact just the 49th to come down uncontrolled since the beginning of the space age [2], and there have been no confirmed casualties due to falling debris from all previous re-entry events. Hence, also the potential danger associated with the falling down of Tiangong-1 was expected to be quite tiny.

Unfortunately, no details about the spacecraft's design, structure and materials were released by China, preventing to know how much of it would have survived the re-entry conditions. However, through comparisons with some monitored re-entries of similar spacecraft (e.g. the ESA's ATV, the Japanese HTV, the Russian Progress and the American Dragon or Cygnus cargo vessels), it could be surmised that a complete demise of Tiangong-1 upon re-entry would have been practically impossible, while a not negligible fraction of the returning mass would have survived and hit the surface of the Earth anywhere in between approximately 44° of North and South latitude. In addition, a possible ground contamination from the extremely toxic propellants still on-board – mono-methyl hydrazine (MMH) and nitrogen tetroxide (N_2O_4) – could not be excluded.

The odds that fragments surviving the fall could cause any damage or injury were, anyway, extremely small. According to experts of the Aerospace Corporation, the individual probability of being hit by a piece of debris from the Chinese space station was less than one in one trillion [3], i.e. much lower than the chance of being hit by lightning. Nevertheless, even if no direct information was available on the possible risk associated with the re-entry of Tiangong-1, the global casualty expectancy for this event was expected to exceed the internationally accepted alert threshold of 10^{-4} by approximately one order of magnitude.

Therefore, as in past events in which the re-entry without control of a manmade space object could have represented a potential threat to people and properties on the Italian territory, the Space Flight Dynamics Laboratory of ISTI-CNR provided support to the Italian Space Agency (ASI) for the National Department of Civil Protection (DPC). It also joined, on behalf of ASI, the re-entry campaign promoted by the Inter-Agency Space Debris Coordination Committee (IADC). The orbital decay of Tiangong-1 was monitored at ISTI-CNR since the beginning of 2017, while a formal re-entry campaign was started in January 2018.

3. Mass before re-entry

An estimation of the mass of Tiangong-1 during its uncontrolled decay phase, following the failure of March 2016, was carried out at ISTI-CNR [4]. Based on openly available information, it was first assumed that the total mass and the propellant mass at launch were 8506 kg and 1000 kg, respectively. The propellant consumption during the mission was calculated starting from the observed changes of the average altitude (Figure 2), leading to estimate a total ΔV of approximately 250 m/s.

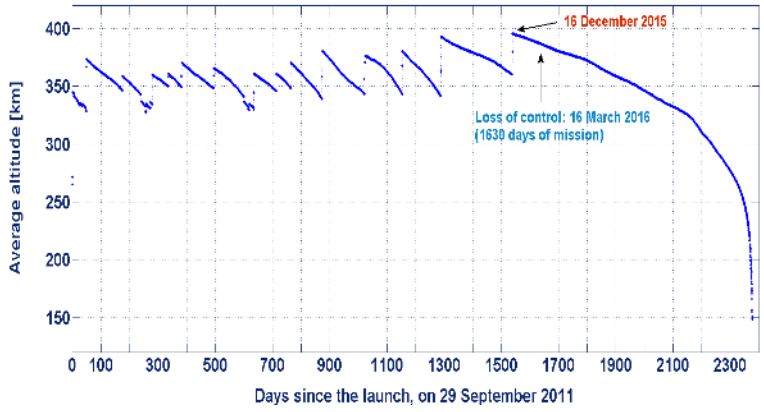

Fig. 2. Evolution of the average altitude of Tiangong-1 since the launch, on 29 September 2011, in which the effects of the main maneuvers are highlighted.

Then, assuming a specific impulse of nearly 336 s for the MMH/N_2O_4 main propulsion system, the corresponding propellant consumption was found to be around 620 kg, rounded off to about 650 kg to include minor maneuvers and attitude control. This estimate left still on board about 350 kg of propellant, including ~120 kg of MMH and ~230 kg of N_2O_4, whose state of aggregation before the re-entry, either liquid or solid, was unknown.

The second step consisted in evaluating the impact of the crews, in terms of spent consumables (e.g. food, water and oxygen) and garbage disposal. In this respect, the following hypotheses were adopted:

- All the consumables needed for the crew stays were pre-loaded on-board the station before launch;
- Toilets were located exclusively in the visiting Shenzhou orbital module;
- Food, water and oxygen consumptions were comparable with those of the International Space Station, with three meals per day;
- The discarded food packages were disposed in the visiting Shenzhou orbital module.

According to these assumptions, each astronaut consumed 5.31 kg/d, including the food packages disposed in the Shenzhou orbital module. Considering the approximately 63 astronaut-days spent on the station, this translated into a mass loss of about 335 kg.

Adding this value to the propellant consumption, the overall mass of Tiangong-1 at the end of the mission was assessed to be around 7500-7550 kg, while its dry mass was estimated to be nearly 7150 kg, or even less, depending on the amount of "fluid" consumables still stored on board.

4. Monitoring the orbital decay

ISTI-CNR began to monitor the orbital decay of Tiangong-1 after the failure occurred in March 2016, when it was clear that the Chinese space station was no longer able to control its orbit, and the vehicle was doomed to a gradual uncontrolled descent towards the Earth.

4.1 Observed orbital decay after the failure

The observed evolution of the spacecraft orbital decay, after the failure of March 2016, was inferred from the US orbit determinations, supplied, for historical reasons, in the so-called NORAD Two-Line Element (TLE) format. Such data, obtained from the Joint Space Operations Center (JSpOC)[*] by processing the observations of the US Space Surveillance Network (SSN), were made available via the Space-Track Organization website [5]. The progress of the space station orbital decay was expressed in terms of its perigee/apogee altitude (Figure 3), average altitude with respect to the Earth's equatorial radius (Figure 4) and semi-major axis decay rate (Figure 5).

Starting from an average altitude (with respect to the Earth's equatorial radius) of approximately 390 km, on 16 March 2016, the spacecraft came down to nearly 250 km in just less than 2 years, on 3 March 2018, reaching the altitude of 200 km about 25 days later, on 28 March 2018, and that of 150 km about 8 hours before re-entry, i.e. on 1 April 2018, at 16:07 UTC (Figure 4).

The decay rate of the semi-major axis was, on average, around 105 m/d from the failure to the end of 2016, and approximately 216 m/d during 2017. It naturally increased approaching the final decay phases,

[*] On 18 July 2018, the Joint Space Operations Center (JSpOC) transitioned to a Combined Space Operations Center (CSpOC) during a ceremony at Vandenberg Air Force Base, in California.

passing from an average of 389 m/d in January 2018, 591 m/d in February, 2.96 km/d in March, up to about 27 km/d during the last two days before re-entry.

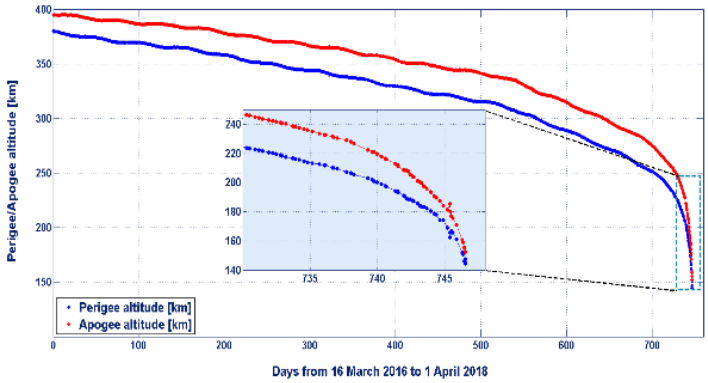

Fig. 3. Observed perigee/apogee altitude evolution of Tiangong-1 from the loss of control, on 16 March 2016, up to about 8 hours before re-entry.

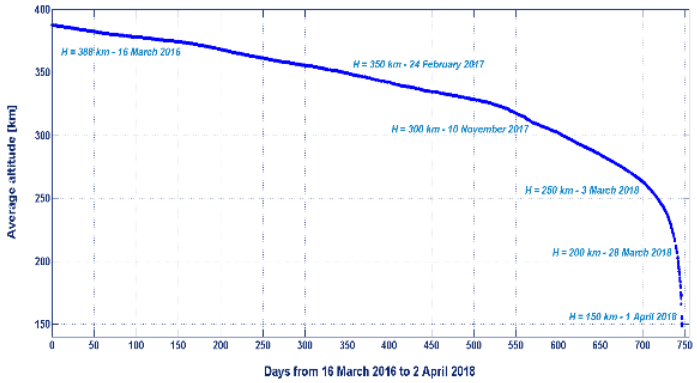

Fig. 4. Observed evolution of the average altitude with respect to the Earth's equatorial radius from the loss of control up to about 8 hours before re-entry.

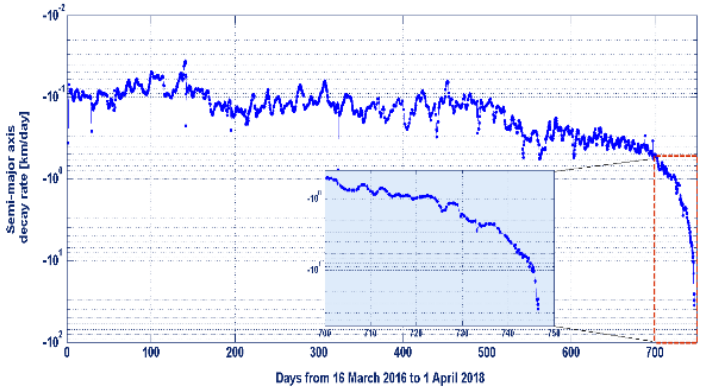

Fig. 5. Observed evolution of the semi-major axis decay rate from the loss of control up to about 8 hours before re-entry.

4.2 Solar and geomagnetic activity conditions

During the period of time following the failure and until the re-entry of Tiangong-1, the environmental conditions were typically characterized by relatively low solar activity levels (Figure 6), with a solar flux at 10.7 cm ($F_{10.7}$), averaged over three solar rotations (81 days), of less than 100 standard flux units ($1\ \text{sfu} = 1 \times 10^{-22}\ \text{W m}^{-2}\ \text{Hz}^{-1}$). Concerning the geomagnetic activity, it was marked by numerous minor (Scale G1, $K_P = 5$) and moderate (Scale G2, $K_P = 6$) geomagnetic storms [6].

The only significant perturbation of the space environment occurred at the beginning of September 2017, when the daily observed $F_{10.7}$ solar flux reached a maximum of 182.5 sfu on 4 September, remaining above 100 sfu from 3 to 10 September (Figure 6). Regarding the geomagnetic activity, a storm approaching the strong level (Scale G3, $K_P = 7$) was recorded on 8 September 2017 ($K_P = 6.6$, $A_P = 106$).

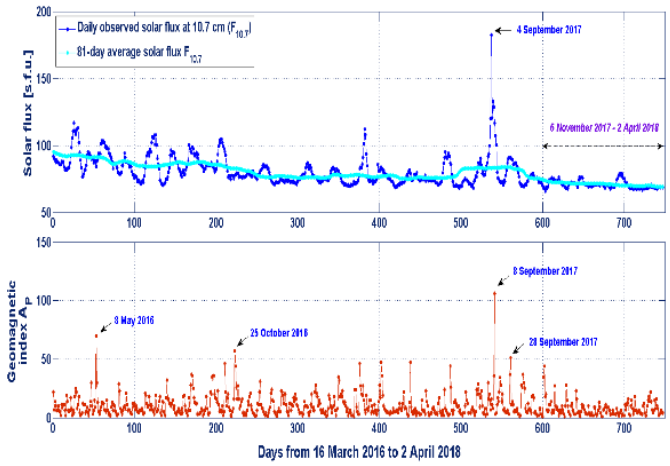

Fig. 6. Solar and geomagnetic activity conditions from the failure to the re-entry of Tiangong-1.

As shown in Figure 6, the last 4.5 months preceding the final decay of Tiangong-1, i.e. approximately from the beginning of November 2017, were characterized by an extremely low solar activity, with an 81-day average $F_{10.7}$ below 75 sfu. Since February 2018, i.e. during the last two months of orbital lifetime, it remained stable below 70 sfu. There were instead numerous G1 geomagnetic storms, which significantly affected the orbit evolution of Tiangong-1, as highlighted by the oscillations observed in its semi-major axis decay rate. As an example, Figure 7 shows an evident correlation between the geomagnetic activity, here expressed in terms of the daily planetary index K_P, and the decay rate, represented by enlarging that presented in Figure 5 in the time span from 28 July 2017 to 14 February 2018.

Greater increases in the decay rate were in fact associated with more disturbed geomagnetic conditions. Effects of similar magnitude were not linked to the evolution of the $F_{10.7}$ solar flux; significant oscillations in the decay rate are indeed also present during periods of very low and stable flux, as occurred since November 2017, while the peak recorded on 4 September 2017 did not correspond to an increased semi-major axis decay rate (see Figure 8).

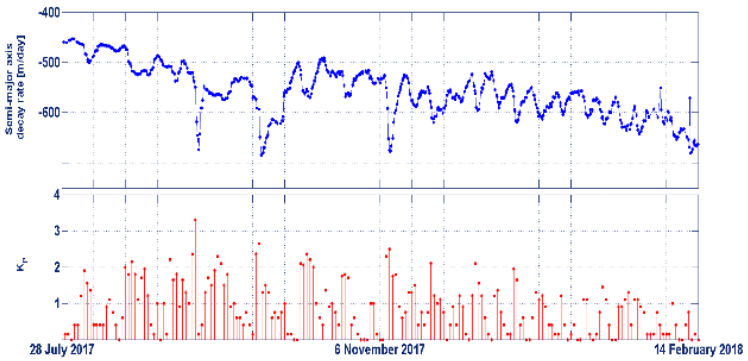

Fig. 7. Correlation between the observed semi-major axis decay rate and the geomagnetic activity from 28 July 2017 to 14 February 2018.

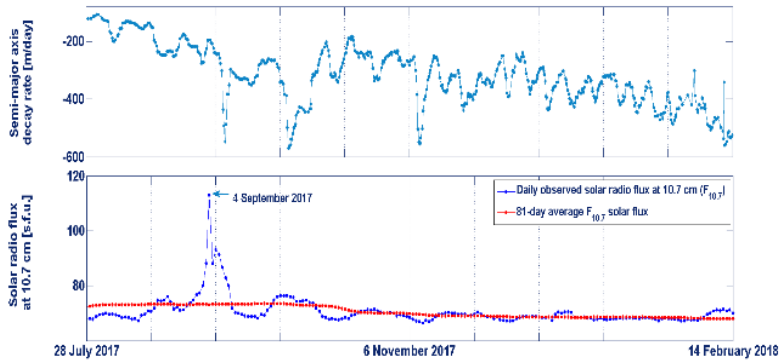

Fig. 8. Evidence of no correlation between the semi-major axis decay rate and the $F_{10.7}$ solar flux from 28 July 2017 to 14 February 2018.

4.3 Residual lifetime estimate

Sparse estimates of the Tiangong-1 residual lifetime were carried out from the beginning of 2017, by progressively intensifying the number of predictions as the final decay phase was approaching. The numerical orbit predictor SATRAP, developed and available at ISTI-CNR [7] [8], was used to propagate the trajectory, while another ISTI-CNR software tool, named CDFIT, was employed to determine the ballistic parameter of the spacecraft, to be used for the propagation. All the main orbit perturbations were shared by both tools, i.e. the geopotential up to 16 × 16 order and degree, the luni-solar attraction, the solar radiation pressure with eclipses and, of course, the aerodynamic drag, were considered in all the predictions carried out. The density of the atmosphere could be computed using one of the nine atmospheric density models implemented in both codes [8], such as NRLMSISE-00 [9], JB2008 [10] or GOST2004 [11].

Estimates of the residual lifetime still far from the final decay, i.e. during 2017 and until February 2018, were performed using the American model NRLMSISE-00 to compute the density of the atmosphere. Since 1 February 2018, also the Russian model GOST2004 was employed for comparison reasons and for checking the mutual consistency of the forecasts.

Concerning the predictions carried out with NRLMSISE-00 during the year 2017 and until the beginning of February 2018 (see Table 1), they systematically obtained a nominal re-entry epoch earlier than the actual one. Therefore, a post-event analysis was performed to investigate whether the cause of the systematic earlier predicted re-entry times was due to a bias in the density model used or to errors in the forecasts of solar and geomagnetic activity.

The second possibility was first verified by replacing the predicted values of the solar and geomagnetic indices with the observed ones, and hence by re-propagating the trajectory under true environmental conditions. In this case, still using NRLMSISE-00 to model the density of the thermosphere, the re-computed nominal re-entry times were indeed delayed with respect to the predictions reported in Table 1, by a percentage of the residual lifetime ranging in between 5% and 7% for the first five predictions, by about 4% for the last but one, and by about 1% for the last one. Therefore, a true representation of the environment would have led to an improvement of the forecasts, by obtaining nominal re-entry times closer to the actual one. However, all the revised predictions adopting the real space weather were still systematically anticipated with respect to the actual re-entry epoch.

Table 1. Nominal re-entry time at 80 km obtained with SATRAP using the density model NRLMSISE-00

Orbit epoch	Predicted re-entry epoch
10 Jan 2017 05:26 UTC	16 Nov 2017 05:55 UTC
16 Nov 2017 02:39 UTC	22 Feb 2018 16:33 UTC
1 Dec 2017 04:05 UTC	28 Feb 2018 17:59 UTC
10 Dec 2017 19:50 UTC	6 Mar 2018 01:09 UTC
18 Dec 2017 04:22 UTC	11 Mar 2018 18:19 UTC
8 Jan 2018 11:22 UTC	22 Mar 2018 02:39 UTC
1 Feb 2018 11:59 UTC	30 Mar 2018 04:17 UTC

The other test consisted in changing the density model used for the thermosphere. For such a posteriori analysis, also the American JB2008 and the Russian GOST2004 models were considered, in addition to NRLMSISE-00, to re-calculate the nominal re-entry times, starting from the orbit epochs given in Table 1. Nevertheless, the three density models were in quite good agreement among them, with a maximum discrepancy, referred to the residual lifetime, of about 9%. Consequently, also their comparison did not allow to solve the problem.

Hence, considering that different density models behaved in a similar way, meaning that, as for NRLMSISE-00, also JB2008 and GOST2004 found a residual lifetime systematically shorter than the actual one, a possible explanation of this result might be that, under the environmental conditions encountered by Tiangong-1 during its uncontrolled decay (i.e. a deep minimum of the solar activity cycle), each atmospheric model analyzed was probably affected by an intrinsic density bias, with a negative derivative with respect to the geodetic altitude, at least down to 270 km. This lead to a percentage increase in the estimation of the atmospheric density as the spacecraft height decreased, neutralizing the absorption of the bias at higher altitudes through the previous ballistic parameter calibrations and causing the systematic underestimation of the residual lifetime recorded up to the beginning of February 2018.

5. Re-entry campaign

Although a few re-entry predictions had been already obtained at ISTI-CNR since the failure of Tiangong-1, in March 2016 (see Section 4.3), the actual re-entry campaign started at the beginning of January 2018 and closed after the plunge of the space station into the Earth's atmosphere, on 2 April 2018.

As highlighted in Section 4.2, the space weather conditions during the campaign were characterized by an extremely low and stable solar activity (Figure 6), and by numerous minor geomagnetic storms (Figures 6 and 9), which significantly affected the orbital evolution of the spacecraft. In fact, it was found that, in similar conditions of solar cycle deep minimum, also minor geomagnetic storms could increase the local thermosphere density by more than 20% at the altitude of the Chinese space station [12]. As a matter of fact, the largest storm, recorded during the night between 18 and 19 March 2018 (Figure 9), was able to move earlier the nominal re-entry of Tiangong-1 by nearly 31 hours [13] [14].

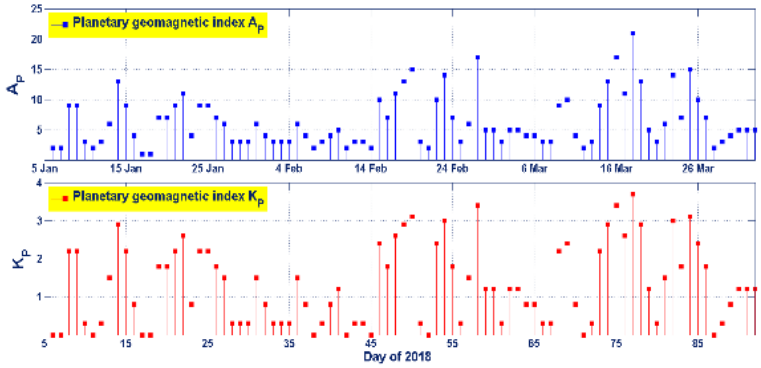

Fig. 9. Geomagnetic activity, in terms of the daily planetary indices A_P (top) and K_P (bottom), during the re-entry campaign for Tiangong-1, from 5 January to 2 April 2018.

5.1 Re-entry predictions

Hundreds of re-entry predictions were performed at ISTI-CNR since January 2018, using various combinations of atmospheric density models, namely NRLMSISE-00 and GOST2004, and time spans for the calibration of the ballistic parameter of the space station, in order to assess the sensitivity and the statistical distribution of the results obtained within a spectrum of reasonable hypotheses [13] [14] [15]. The density model NRLMSISE-00 was used from the beginning of the campaign, while the use of GOST2004 started on 1 February 2018, to compare its predictions with those obtained with NRLMSISE-00. Moreover, not all the forecasts made with the American model were repeated with the Russian one.

From the beginning of February, i.e. when the mean altitude with respect to the equatorial radius of the Earth descended below 270 km, the nominal re-entry time began to converge towards the first week of April 2018 (Figures 10, 11 and 12). However, the largest geomagnetic storm recorded during the campaign, occurred in the night between 18 and 19 March, caused a significant advance, shifting the distribution of nominal re-entry predictions to the days from 30 March to 3 April 2018 (Figure 13).

Starting 21 March 2018, the nominal re-entry epoch settled on 1 April 2018. To be exact, in a 24-hour period between 01:00 UTC of 1 April and 01:00 UTC of 2 April. Within this 24-hour interval, the only important shift occurred since 30 March, when an unusually long period of quiet geomagnetic conditions led to a cooling down of the atmosphere, with a consequent reduction of the density and a progressive delay of the Tiangong-1 expected re-entry (Figure 14).

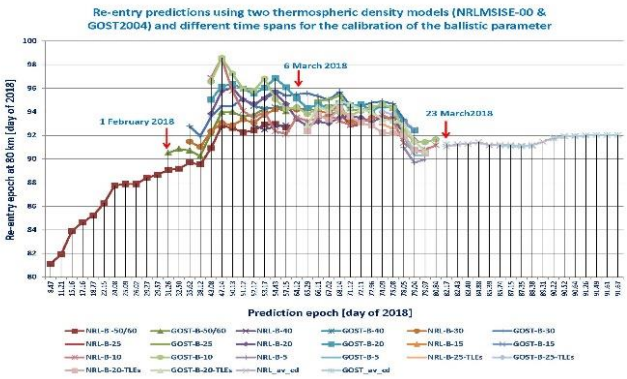

Fig. 10. Nominal re-entry predictions obtained with two atmospheric density models, NRLMSISE-00 and GOST2004, and different time spans for the calibration of the ballistic parameter.

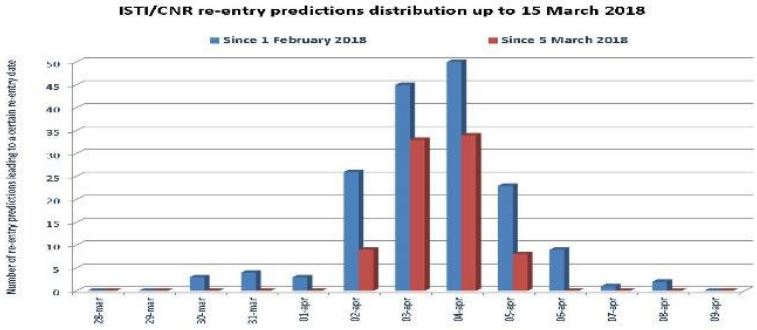

Fig. 11. Distribution of the nominal re-entry predictions of ISTI-CNR until 15 March 2018 (since 1 February 2018, in blue, and since 5 March 2018, in red); they resulted from various combinations of two atmospheric density models, NRLMSISE-00 and GOST2004, and time spans for calibrating the ballistic parameter of Tiangong-1.

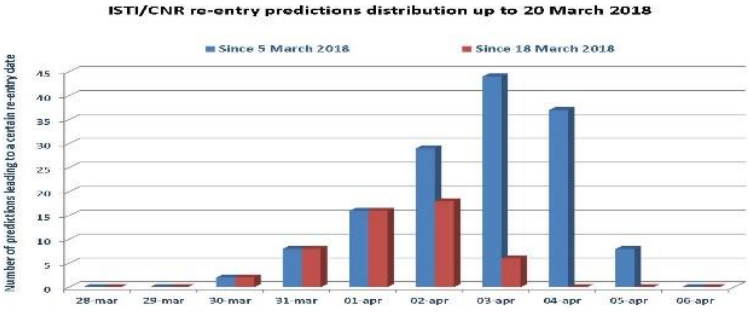

Fig. 12. Distribution of the nominal re-entry predictions made by ISTI-CNR until 20 March 2018, using both NRLMSISE-00 and GOST2004 (since 5 March 2018, in blue, and since 18 March 2018, in red).

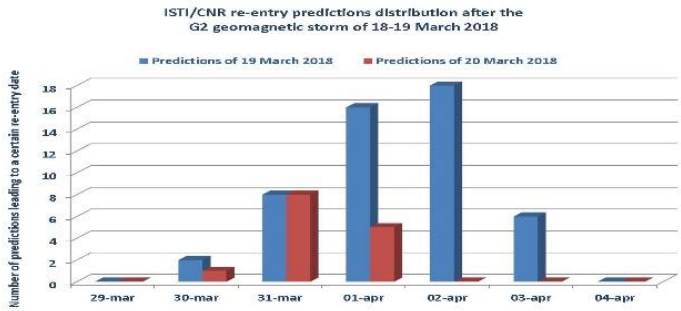

Fig. 13. Distribution of the nominal re-entry predictions of ISTI-CNR after the geomagnetic storm occurred in the night of 18-19 March 2018 (predictions made on 19 March, in blue, and on 20 March, in red).

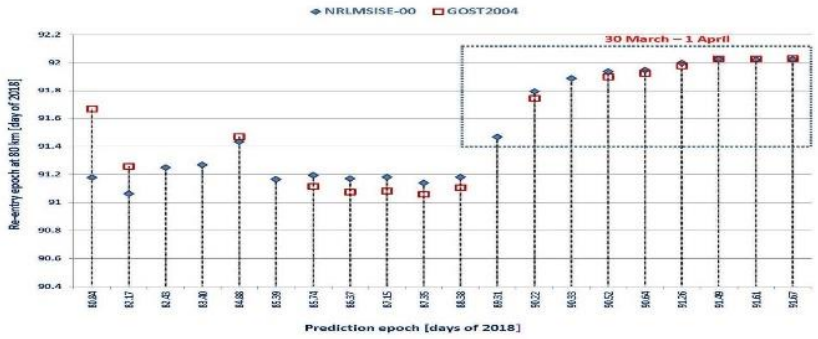

Fig. 14. ISTI-CNR nominal re-entry predictions since 21 March 2018, during the period of relatively quiet geomagnetic conditions (in particular in the final six days of orbital lifetime) which followed the geomagnetic storm of 18-19 March.

5.2 Re-entry uncertainty windows

Even when the best practices are adopted and the best data available are used, there are still specific error sources directly linked to the drag modeling. These include, among others: the error in the estimation of the ballistic parameter of the re-entering object, as well as the uncertainty in its evolution; the uncertainties affecting the solar and geomagnetic activity forecasts; and the biases and the stochastic errors affecting the atmospheric density models. Therefore, defining a reliable and conservative uncertainty window has always been a very challenging task.

There are no standard criteria to proceed, but a reasonable approach is to take advantage of the expertise gained during a sufficiently high number of past re-entry events. Recently, an extensive analysis was carried out to quantify the global impact of the above mentioned error sources, based on operational prediction campaigns starting 10-15 days before re-entry, and spanning a wide range of object types and space weather conditions [16]. In general, a relative error, in the residual lifetime, of $\pm 20\%$ includes nearly 90% of the cases, while a relative error of $\pm 30\%$ almost includes 95% of them. Hence, considering that the re-entry uncertainty windows for Tiangong-1 should have been used for civil protection applications, they were defined in order to guarantee a confidence level of at least 95%. This was obtained by either decreasing and increasing the nominal residual lifetime of the spacecraft by 30%. Such an

approach proved to be fully adequate, despite the complexity of the vehicle dynamics and environmental conditions, and none of the re-entry uncertainty windows so obtained was violated by the post-event reference re-entry epoch (Figure 15).

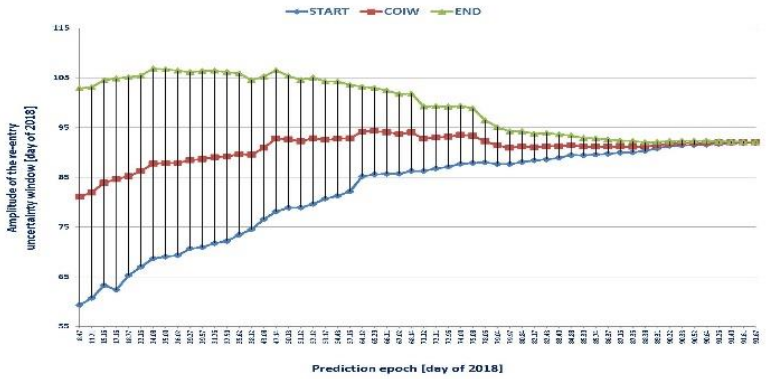

Fig. 15. ISTI-CNR re-entry uncertainty windows for Tiangong-1 associated with the predictions performed during the re-entry campaign, from 8 January to 2 April 2018; for each prediction (in brown), the blue point identifies the opening and the green point the closure of the corresponding uncertainty window.

5.3 Ballistic parameter evolution

An essential aspect of the re-entry prediction process was represented by the determination of the spacecraft ballistic parameter, $B = C_D \times A/M$, in terms of its drag coefficient C_D and area-to-mass ratio A/M. Updated estimates of B, based on the fit of the observed orbital decay of Tiangong-1, were obtained with both density models, NRLMSISE-00 and GOST2004. The first one was used since the beginning of the re-entry campaign, on 8 January 2018, the second starting from 1 February 2018. The evolution of the ballistic parameter determined with NRLMSISE-00 is shown in Figure 16, while the comparison of the results obtained with both models is plotted in Figure 17.

The value of B determined with NRLMSISE-00 (see Figure 16) steadily decreased by more than 15% in January and February 2018, increased back to the value at the beginning of the campaign, in March, and then remained basically stable until the end of the month. Hence, it finally dropped abruptly by more than 20% during the last 3 days in orbit. The average value of the ballistic parameter, obtained with NRLMSISE-00 during the re-entry campaign, was 0.007388 m^2/kg, with a standard deviation $\sigma = 6.698\%$ ($3\sigma \approx 20\%$). Concerning the comparison between the results obtained with the two density models (see Figure 17), it is clear that, in spite of some gaps in the evolution of B in the case of GOST2004, due to the fact that not all predictions were repeated using this model, both show a similar behavior. However, it is also evident that a bias exists between the two models, and, at least under the environmental conditions encountered during the re-entry campaign of Tiangong-1, GOST2004 systematically found a thermospheric density higher than NRLMSISE-00.

Even though, from an operational point of view, the updated determinations of B obtained by fitting the observed semi-major axis decay provided the right information needed to characterize the state of the spacecraft at the beginning of each re-entry prediction, it would be worthwhile to discuss as well the reasons leading to the observed changes of the ballistic parameter shown in Figures 16 and 17. According to the definition of B, the most obvious causes of change may be a variation of A/M and/or of C_D. In the case of Tiangong-1, the mass M was probably constant, while A depended on the attitude evolution of the

space station. The drag coefficient was instead affected by the molecular flow regime and by the orientation of the spacecraft with respect to the air flow. However, being the atmospheric drag a function of the product between B and the air density, any error in the model used to describe the atmospheric density affects the estimate of the ballistic parameter. Therefore, the changes of B may be due not only to the variation of spacecraft attitude and drag coefficient, but also to the errors affecting the modeling of the atmospheric density at the altitude of Tiangong-1.

The first suspect cause of change of B was obviously a variation of the average cross-section A, perpendicular to the flight velocity with respect to the atmosphere. Unfortunately, both during the re-entry campaign and afterwards, we had no access to the JSpOC radar cross-section history. The only information available on the Tiangong-1 attitude motion, published nearly 10 months after the re-entry, was found in [17]. The German Tracking and Imaging Radar (TIRA) regularly monitored Tiangong-1 from 9 February 2017 to 1 April 2018. In inertial coordinates, the rotation axis preceded roughly in a plane, describing nearly half a circle, while the angular velocity increased from 0.18°/s to 3.6°/s. Since January 2018, the spacecraft was found rotating approximately around the principal axis of inertia. During three passes, it was also possible to estimate the average cross-section A: it was 65 m^2 on 9 February 2017, 40 m^2 on 11 February 2018, and 26 m^2 on 1 April 2018. From these estimates, a progressive decrease of the effective cross-section was deduced [17]. However, if such conclusions were true, the results displayed in Figures 16 and 17 would clearly indicate that the variation of A was not able, taken alone, to explain the observed changes of B. In fact, B increased when it should have decreased along with A or, based on the TIRA average cross-section estimates, it was higher than expected, by at least 30%, on 1 April 2018, assuming as reference the value found on 11 February 2018.

Concerning the B sharp drop observed during the last three days, at least part of it might be due, in principle, to the C_D decrease caused by the transition from a purely free molecular flow regime, characterized by a Knudsen number $Kn > 10$, to a transitional rarified regime, with $0.01 < Kn < 10$ [18]. However, in the case of Tiangong-1, the free molecular flow regime applied down to a geodetic altitude of approximately 165 km, i.e. up to 24 hours before re-entry. Therefore, more than 2/3 of the B decrease observed during the last three days was recorded when Tiangong-1 was still in the free molecular flow regime. In addition, during the last day, after a further decrease of B by 6%, the ballistic parameter remained basically the same up to 9 hours before re-entry, when the geodetic altitude was around 150 km and the last determination of B was obtained.

Hence, having excluded a substantial correlation between the observed evolution of B and the variation of the cross-sectional area and drag coefficient of Tiangong-1, it could reasonably be presumed that significant biases of the density models, linked to low solar activity levels as well as to the sequence of minor geomagnetic storms, likely played a major role in producing the observed changes of B, both above and below 165 km. This was probably the case, in particular, for the major increase of B after the storm of 18-19 March, or for the drop that occurred in the three days of decidedly quiet geomagnetic conditions preceding the final decay.

Fig. 16. Evolution of the Tiangong-1 ballistic parameter determined at ISTI-CNR with the density model NRLMSISE-00.

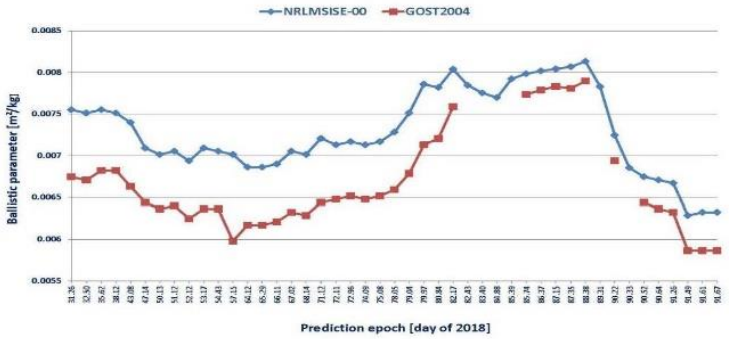

Fig. 17. Comparison of the Tiangong-1 ballistic parameter evolutions obtained at ISTI-CNR with NRLMSISE-00 (top) and GOST2004 (bottom), from 1 February 2018 to re-entry.

5.4 IADC re-entry campaign

Tiangong-1 was also selected as the test object for the re-entry campaign promoted by the Inter-Agency Space Debris Coordination Committee in 2018. This was the 22nd IADC campaign since the first one, in October 1998, which targeted the small spacecraft Inspector [16]. An IADC re-entry exercise allows the timely exchange of technical information, i.e. orbit determinations, re-entry predictions, various satellite data, documents and plots, among the participating members, by means of a digital network and a database, which were established and are still maintained at the European Space Operations Centre (ESOC) of the European Space Agency (ESA), in Darmstadt, Germany. The main objective of these campaigns is to promote a close international cooperation, in order to maintain and guarantee an adequate level of operational readiness to deal with any foreseeable re-entry emergency.

As for all the previous IADC re-entry exercises, also in the Tiangong-1 case ISTI-CNR participated on behalf of the Italian Space Agency (ASI). The activity officially started on 15 February and ended after the re-entry of the space station, on 2 April 2018. It was the longest IADC re-entry campaign ever, having lasted just more than 1 month and a half (47 days). During the IADC campaign, ISTI-CNR officially issued 24 re-entry predictions with the associated uncertainty windows (they were just a small selected subset of the forecasts made during the overall ISTI-CNR re-entry campaign, started in January 2018), having initial orbit epochs from 14 March (the first one) to 1 April (the last one). In addition to being provided to the IADC member agencies, these official forecasts were issued as well to the Italian Space

Agency and to the National Department of Civil Protection.

Thanks to the IADC data exchange and re-entry database [19], since 26 February 2018, in addition to the 116 TLEs provided by the US Space Surveillance Network, 140 TLEs were supplied by the Russian Space Surveillance System, 10 by the German Space Agency (DLR) and 9 by ESA through the TIRA radar, and 2 by the Italian Ministry of Defense through the MFDR-MR radar [15].

The maximum relative error affecting the ISTI-CNR predictions for the IADC campaign was 22%, 3.64 days before re-entry, due to the previously mentioned unexpected deep cooling of the atmosphere that occurred in the last few days. The mean prediction error during the campaign was less than 10%, around 6% in the last 48 hours, and around 4% during the last 24 hours (Figure 18).

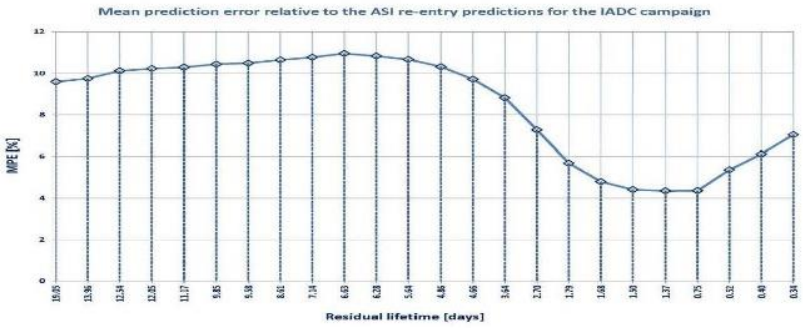

Fig. 18. ISTI-CNR running mean prediction errors (MPE) during the IADC re-entry campaign.

5.5 Final sub-satellite ground tracks

The ground tracks included in the last three uncertainty windows issued by ISTI-CNR are shown in Figures 19, 20 and 21. A posteriori, it was possible to verify that the orbit in which the re-entry would have taken place had been already identified 15 hours before (Figure 19), but unfortunately the a priori uncertainty was still large, at that time, and included 3 risky passes over parts of Italy.

The situation did not radically improve with the prediction issued 9.5 hours before re-entry (Figure 20), in particular because a critical pass was still present (Figure 22). Only with the last prediction, issued 5 hours before re-entry (Figure 21), the Italian territory was mostly excluded from any residual risk, with the exception of some small islands in the middle of the Mediterranean Sea (Figure 23). Due to the lack of further orbit determinations during the last 8 hours of flight, no subsequent re-entry prediction was possible and a few Italian islands, a portion of territorial waters and the overhead air space remained in the risk window until the end (Figure 23).

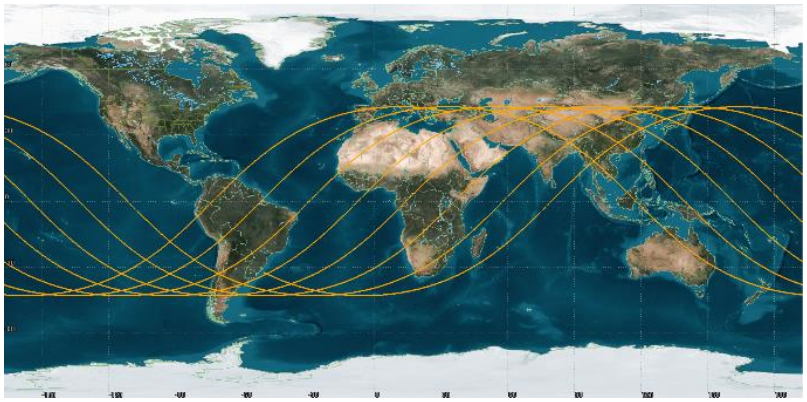

Fig. 19. Tiangong-1 ground track included in the uncertainty window issued by ISTI-CNR almost 15 hours before re-entry.

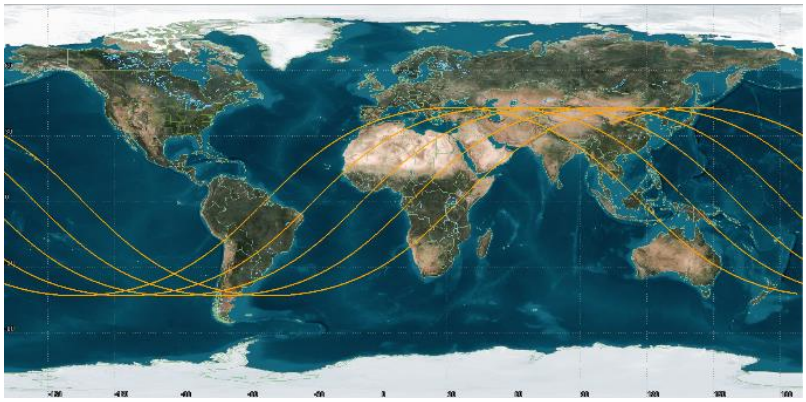

Fig. 20. Tiangong-1 ground track included in the uncertainty window issued by ISTI-CNR about 9.5 hours before re-entry.

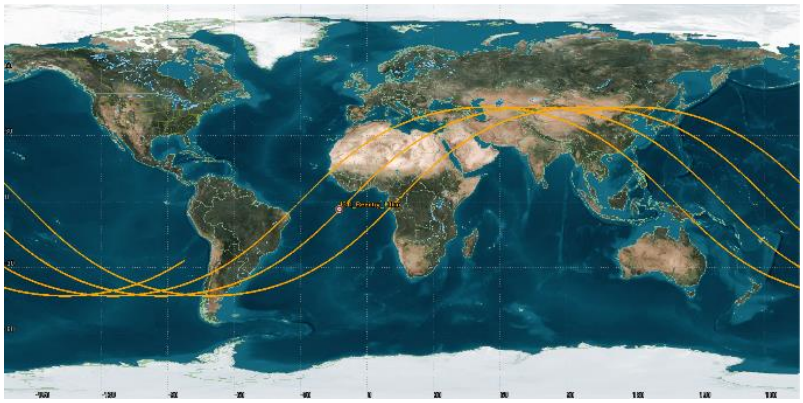

Fig. 21. Tiangong-1 ground track included in the uncertainty window issued by ISTI-CNR about 5 hours before re-entry.

Fig. 22. Ascending re-entry track over Italy (central line) still included in the global uncertainty window 9.5 hours before the Tiangong-1 orbital decay; the corresponding alert time window for possible debris crossing the Italian airspace, or impacting the ground, was 3:58–4:28 UTC on 2 April 2018, and the cross-track swath was ± 100 km.

Fig. 23. Ascending re-entry track over Italy (central line) still included in the global uncertainty window 5 hours before the Tiangong-1 orbital decay; the corresponding alert time window for possible debris crossing the Italian airspace, or impacting the ground, was 2:25–2:55 UTC on 2 April 2018, and the cross-track swath was ± 100 km.

5.6 Tiangong-1 re-entry assessment

According to the last ISTI-CNR prediction, made using the last available American TLE of 16:07 UTC, on 1 April 2018, the nominal re-entry of Tiangong-1, at the geodetic altitude of 80 km, would have occurred on 2 April 2018, at 00:44 UTC. The associated uncertainty window had a width of ± 2.62 hours. It included the post-event assessment released by JSpOC after the orbital decay, indicating that the object would have reached the altitude interface of 80 km at 00:10 UTC ± 1 minute, on 2 April 2018, i.e. just 34 minutes earlier than the last ISTI-CNR forecast and not far from the originally targeted SPOUA, in the middle of the southern Pacific Ocean, as shown in Figure 24.

However, in the 8 hours that preceded the re-entry, the US SSN could not make any new orbit determination and the final assessment issued by JSpOC seems the result of two further "refinements" of the last "old" orbital solution, in which the ballistic parameter of the object was at the end increased, then

anticipating its fall. Moreover, unlike what often happens in similar cases, it does not seem that the Tiangong-1 re-entry had been observed in the infrared by the classified satellites used for the real-time monitoring of ballistic missile launches. Further complicating the situation is the fact that the Russian Space Surveillance System issued, after the re-entry, a latest orbit determination obtained with the tracking data acquired during the final pass of Tiangong-1 over the Russian radar sensors, when the object was already traveling along the last orbit and was just 125 km high.

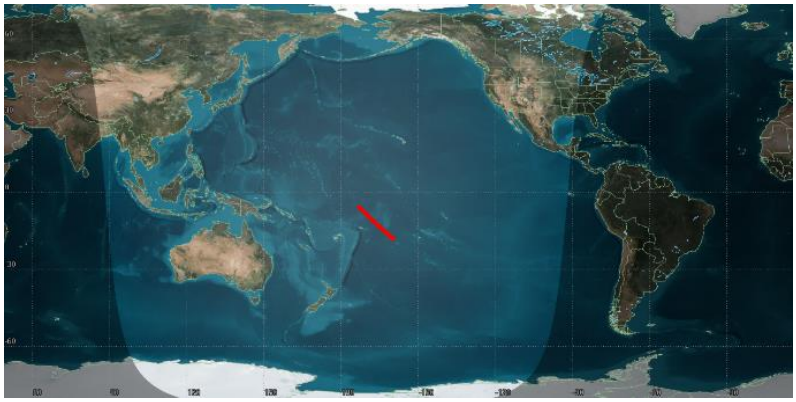

Fig. 24. Area of possible dispersion of the fragments of Tiangong-1 if the post-re-entry assessment issued by JSpOC was correct.

Well, using this last Russian TLE, it would be impossible to obtain a re-entry in agreement with that of JSpOC [20]. So, either the last Russian orbit determination was wrong, and the re-entry actually took place in the Pacific Ocean, as found by JSpOC, or it occurred in the southern Atlantic Ocean, between Uruguay and the Island of Ascension, as found by the Russians. Figure 25 shows the post-re-entry estimates obtained by Roscosmos and ISTI-CNR, using the last Russian TLE, compared with the post-event assessment issued by JSpOC. It should be remarked that the solution obtained by Roscosmos remained compatible with the fact that the Ascension radar station did not reacquire Tiangong-1, this "no-show" being the first real-time confirmation of the occurred re-entry.

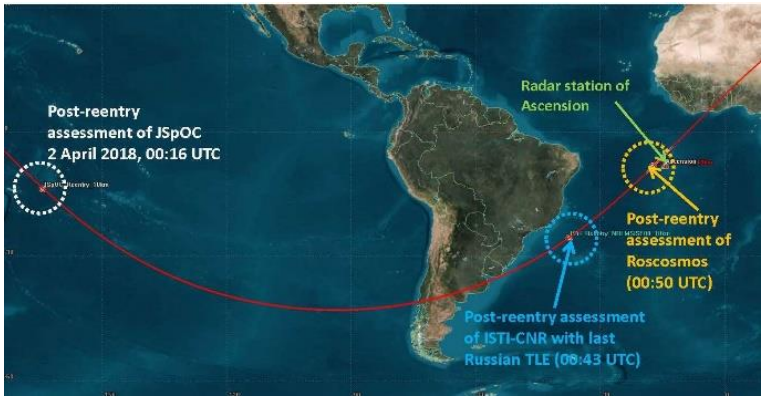

Fig. 25. Post-re-entry estimates (at the geodetic height of 10 km) by Roscosmos and ISTI-CNR, based on the latest Russian TLE, compared with that of JSpOC, based on the latest American TLE.

Considering the reference geodetic altitude of 80 km and adopting the latest Russian TLE, the Roscosmos estimate placed the Tiangong-1 re-entry at 00:44 UTC, on 2 April 2018. This prediction was identical to the last forecast issued by ISTI-CNR using the last available American TLE of 16:07 UTC, on 1 April 2018. Instead, using the final Russian TLE, ISTI-CNR obtained a nominal re-entry at 00:37 UTC, which was just 7 minutes earlier than Roscosmos, but 27 minutes later than JSpOC.

On the other hand, a sighting of the re-entry was indeed reported from the Tahiti Island, in the Pacific Ocean [21]. Based on that, Nazarenko and Usovik came to the conclusion that the re-entry of Tiangong-1 had occurred a few minutes after the JSpOC assessment [21]. However, such a sighting remained an isolated claim without further authentication of the source reliability, and no independent and credible video or image of the re-entry has been reported, so far, to solve this puzzle. Therefore, in our opinion, the actual re-entry epoch of Tiangong-1 stays unconfirmed.

6. Acknowledgements

The work described in this paper was carried out in the framework of the Agreement No. 2015-028-R.0 between ASI and INAF (National Institute of Astrophysics). The authors would also like to thank Andrey I. Nazarenko and Vasiliy Yurasov for their precious and irreplaceable advice and cooperation during the Tiangong-1 re-entry campaign (http://www.satmotion.ru/cntnt/eng/o-sayte-eng/news/decay-epoch-of-the-tiangong-1-sp.html).

7. References

[1] Permanent Mission of China to the United Nations. Note dated 4 May 2017 addressed to the Secretary-General, United Nations General Assembly, A/AC.105/1150, 10 May 2017, reissued for technical reasons on 30 June 2017, Committee on the Peaceful Uses of Outer Space (COPUOS), Vienna, Austria.

[2] McDowell, J. (2018). The Biggest Uncontrolled Reentries (last modified on 30 March 2018), http://planet4589.org/space/misc/big_reentries.txt.

[3] Aerospace Corporation (2018). Chinese Space Station Return (last modified on 9 May 2018), https://aerospace.org.

[4] Pardini, C. & Anselmo, L. (2018). Estimate of Tiangong-1 Mass at Reentry, Space Flight Dynamics Laboratory Memo for the Reentry Campaign IADC-2018-1, TG-1 ISTI-CNR Memo-01, Pisa, Italy.

[5] Space-Track Organization (2018). Two-Line Element (TLE) Sets of Tiangong-1 (last accessed on 3 April 2018), http://www.space-track.org.

[6] National Oceanic and Atmospheric Administration (2018). NOAA Space Weather Scales (accessed on 30 March 2018), http://www.swpc.noaa.gov/noaa-scales-explanation.

[7] Pardini, C. & Anselmo, L. (1994). SATRAP: Satellite Reentry Analysis Program, Internal Report C94-17, CNUCE Institute, CNR, Pisa, Italy.

[8] Pardini, C., Moe, K. & Anselmo, L. (2012). Thermospheric Density Model Biases at the 23rd Sunspot Maximum, Planet. Space Sci. 67, 130–146.

[9] Picone, J.M. & al. (2002). NRLMSISE-00 Empirical Model of the Atmosphere: Statistical Compari-sons and Scientific Issues, J. Geophys. Res. 107, 1468.

[10] Bowman, B.R. & al. (2008). A New Empirical Thermospheric Density Model JB2008 Using New Solar and Geomagnetic Indices, AIAA/AAS Astrodynamics Specialist Conference, Honolulu, Hawaii, USA, Paper AIAA 2008-6438.

[11] Volkov, I.I. (2004). Earth's Upper Atmosphere Density Model for Ballistic Support of the Flight of Artificial Earth Satellites, GOST R 25645.166-2004, Publishing House of the Standards, Moscow, Russia.
[12] Vellutini, E. & al. (2018). Monitoring the Final Orbital Decay and the Re-entry of Tiangong-1 with the Italian SST Ground Sensor Network, 69th International Astronautical Congress, Bremen, Germany, Paper IAC-18-A6.7.7.
[13] Pardini, C. & Anselmo, L. (2018). The Uncontrolled Re-entry of Tiangong-1, Presentation at the 36th IADC Plenary Meeting, International Congress Center, Tsukuba, Japan.
[14] Pardini, C. & Anselmo, L. (2018). Uncontrolled Re-entries of Sizable Spacecraft and Rocket Bodies: A Potential Threat in the Airspace and on the Ground, 42nd COSPAR Scientific Assembly, Pasadena, California, USA, Presentation PEDAS.1-0012-18.
[15] Anselmo, L. & Pardini, C. (2019). Uncontrolled Reentries: Characterization, Monitoring, Predictions and Operational Procedures for Civil Protection Applications, Version 1.1, ISTI Institute, CNR, Pisa, Italy.
[16] Pardini, C. & Anselmo, L. (2018). Assessing the Risk and the Uncertainty Affecting the Uncontrolled Re-entry of Manmade Space Objects, J. Space Safety Eng. 5, 46–62.
[17] Sommer, S. & al. (2019). Analysis of the Attitude Motion and Cross-sectional Area of Tiangong-1 During its Uncontrolled Re-entry, 1st NEO and Debris Detection Conference, ESA Space Safety Programme Office, Darmstadt, Germany.
[18] Koppenwallner, G. (2013). Aerodynamic Flow Regimes, in Sgobba, T. & al. (Eds.), Safety Design for Space Operations, Elsevier Ltd., Amsterdam, The Netherland, pp. 615–617.
[19] ESA European Space Operations Centre (2018). IADC Re-entry Database (last modified on 3 April 2018), https://iadc-redb.esoc.esa.int/iadcredb/REDBWeb.html.
[20] Pardini, C. & Anselmo, L. (2019). Uncontrolled Re-entries of Spacecraft and Rocket Bodies: A Statistical Overview over the Last Decade, J. Space Safety Eng. 6, 30–47.
[21] Nazarenko, A.I. & Usovik, I.V. (2019). The Effect of Parameters of the Initial Data Updating Algorithm on the Accuracy of Spacecraft Reentry Time Prediction, J. Space Safety Eng. 6, 24–29.